THE ANNALS "DUNĂREA DE JOS" UNIVERSITY OF GALAŢI
FASCICLE V, TECHNOLOGIES IN MECANICAL ENGINEERING,
ISSN 1221-4566, 2018
https://doi.org/10.35219/tmb.2018.1.06

COMPARATIVE STUDY REGARDING TWO CONSTRUCTIVE SOLUTIONS FOR CONICAL WORM FROM PUMP CONSTRUCTION

Nicuşor BAROIU[1], Virgil Gabriel TEODOR[1],
Viorel PĂUNOIU[1], Nicolae OANCEA[1]

[1] Department of Manufacturing Engineering, „Dunărea de Jos" University of Galați, România
Nicusor.Baroiu@ugal.ro

ABSTRACT

In this paper two constructive solutions for central conical worm from composition of helical compressor are analyzed. First is a worm with cycloid frontal profile and the second one is a worm with circle arc frontal profile. The conjugated worm for the conical rotor is determined based on the fundamental theorems of surface enwrapping. Afterward, the area between the flanks of lobes for drive and driving worms are calculated in sections perpendicular to the axis of driving worm.

For equals dimensions of worms it is estimated the volume included between the drive and driving worms, as determining factor defining the compressor flow.

KEYWORDS: conical worm, helical compressor, enwrapping surfaces

1. INTRODUCTION

Helical compressors were firstly created by Sheldon S.L. Chang [1]. As industrial applications were introduced by O. Dmitrev and I. Arbon, which, together with the leaded team founded a specific industry, imposed this compressors type in various industrial applications [2], [3], [4], [5].

In this paper is proposed an analysis based on an analytical development of two constructive forms for the included worm: conical worm with cycloid frontal profile and conical worm with frontal profile in circle arc.

The analytical forms for both conical worms were developed in order to assess the area included between the lobes of including and included worms. The areas are regarded as fundamental geometric parameter for the estimation of the fluid flow for this compressor type. In the analysis were used the fundamental theorem of surface enwrapping [6], [7] and also were used the capabilities of CATIA design environment, [8].

For the determining of conjugated profile of the worm with frontal profile in circle arc were using the in-plane trajectories method [9].

The geometric values of spaces included in crossing sections for these compressor types were assessed.

2. CONSTRUCTIVE SOLUTION FOR WORM WITH FRONTAL PROFILE IN CIRCLE ARCS

2.1. Frontal profile of included worm

A conical worm with frontal profile in circle arcs was analysed. The frontal profile of the worm is composed by a circle arcs assembly, filled one each other, see figure 1.

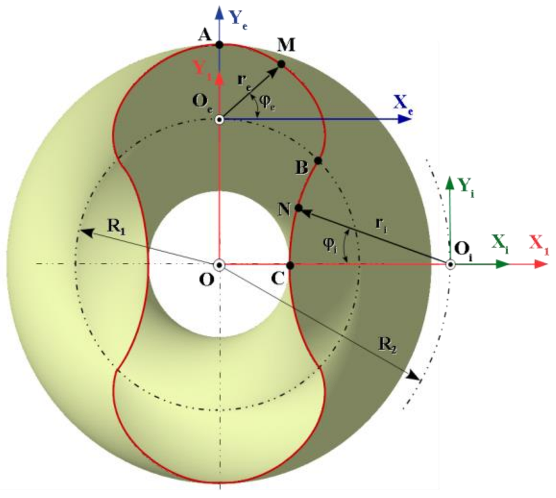

Fig. 1. *Crossing profile of the worm with lobes – circles arcs*

The frontal profile of the worm is composed by an assembly of circle arcs with r_e and r_i radii, with centres O_e and O_i. The arcs $\overset{\frown}{AB}$ and $\overset{\frown}{BC}$ compose the half profile of the worm lobe, for the case of two lobes worm.

They are defined the references systems:

- X_eY_e – mobile reference system joined with the convex lobe;
- X_iY_i – mobile reference system joined with concave lobe;
- $X_1Y_1Z_1$ – reference system joined with the conical worm (Z_1), with centre in point O.

Note: With $X_2Y_2Z_2$ will be denoted the reference system joined with the including worm.

The current coordinates on the two circles are defined as:

$$\overset{\frown}{AB}\ \left| \begin{aligned} &X_1 = r_e \cdot \cos\varphi_e; \\ &Y_1 = r_e \cdot \sin\varphi_e + R_1; \end{aligned} \right. \qquad (1)$$

$$\overset{\frown}{BC}\ \left| \begin{aligned} &X_1 = -r_i \cdot \cos\varphi_i + R_2; \\ &Y_1 = r_i \cdot \sin\varphi_i . \end{aligned} \right. \qquad (2)$$

The two circle arcs are regarded as tangents in point B, see figure 1.

2.2. Helical conical flank of the included worm

In figure 2 is presented the crossing section of the conic support of worm's lobes, with radius variable along the worm's axis, in limits $R = R_O$, initial section and $R = R_L$ in final section of the worm.

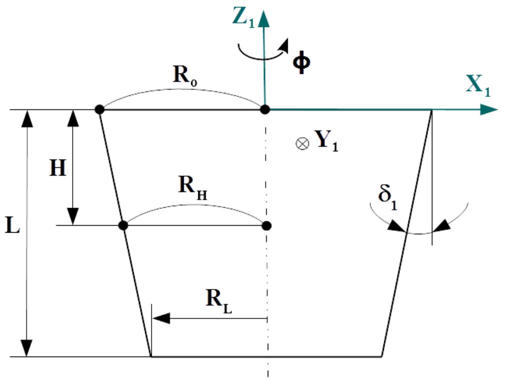

Fig. 2. *Crossing section of conical support of helical flanks*

It is acceptable that the R radius is variable along the worm's axis, see figure 1:

$$R = R_O - p\cdot\phi\cdot tg\delta_1 \qquad (3)$$

where: p represents the helical parameter; δ_1 generatrix angle of the support cone for helical lobes.

Similarly, the radii values for frontal circles of conical lobes:

$$\begin{aligned} &r_e = r_{Oe} - p\cdot\phi\cdot tg\delta_1; \\ &r_i = r_{Oi} - p\cdot\phi\cdot tg\delta_1, \end{aligned} \qquad (4)$$

with Φ angular parameter.

In these conditions, the flanks surfaces equations can be determined, see (1) and (2):

$$\Sigma_{AB} \left| \begin{aligned} &X_1 = r_e\cdot\cos\varphi_e\cdot\cos\phi - \\ &-\left(r_e\cdot\sin\varphi_e + R_1\right)\cdot\sin\phi; \\ &Y_1 = r_e\cdot\cos\varphi_e\cdot\sin\phi + \\ &+\left(r_e\cdot\sin\varphi_e + R_1\right)\cdot\cos\phi; \\ &Z_1 = p\cdot\phi, \end{aligned} \right. \qquad (5)$$

respectively,

$$\Sigma_{BC} \left| \begin{aligned} &X_1 = \left(-r_i\cdot\cos\varphi_i + R_2\right)\cdot\cos\phi - \\ &-r_i\cdot\sin\varphi_i\cdot\sin\phi; \\ &Y_1 = \left(-r_i\cdot\cos\varphi_i + R_2\right)\cdot\sin\phi + \\ &+r_i\cdot\sin\varphi_i\cdot\cos\phi; \\ &Z_1 = p\cdot\phi, \end{aligned} \right. \qquad (6)$$

with R_1, R_2, r_e and r_1 variable values, defined by, (3) and (4).

2.3. Including worm of conical helical compressor

The including worm, see figure 3, is associated with a conical surface, with axis $\vec{V}_2(Z_2)$, intersecting the axis $\vec{V}_1(Z_1)$, of the included surface (driving conical worm of the conical helical compressor), in point O_0.

They are defined the reference systems:

- $X_1Y_1Z_1$ – mobile reference system joined with the included worm; Z_1 axis is the axis of cone with R_0 radius and δ_1 half angle;
- $X_2Y_2Z_2$ – mobile reference system joined with the axis of including cone, with axis Z_2 and δ_2 half angle.

They also defined the fixed reference systems:

- $x_1y_1z_1$ $\vec{V}_1(Z_1)$ - with axes $\vec{V}_1$ and Z_1 overlapped;
- $x_2y_2z_2$ $\vec{V}_2(Z_2)$ - with axes $\vec{V}_2$ and Z_2 overlapped.

They are defined the relations:

$$L = \frac{R_1}{\sin\delta_1} = \frac{R_2}{\sin\delta_2}, \qquad (7)$$

where L is the length of common generatrix of cones with axes $\vec{V}_1$ and $\vec{V}_2$;
- $R_1 = R_o$, see definition (3).

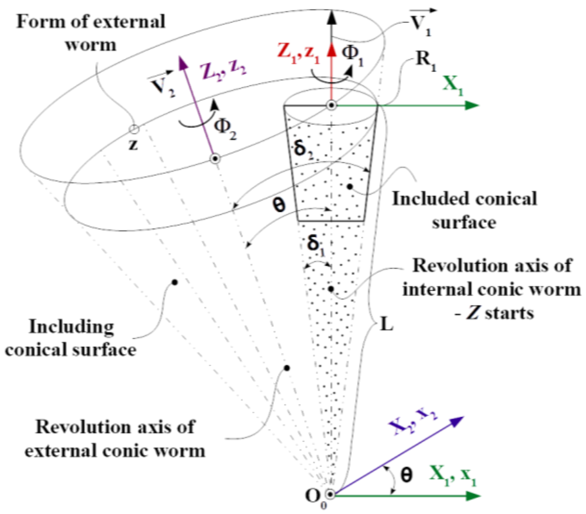

Fig. 3. *Conical surfaces of included and including worms of conical helical compressor*

If the rotation angles, in the rolling process of the two conical surfaces, are denoted with Φ_1 and Φ_2, then the gearing ratio is:

$$i_{1,2} = \frac{\phi_2}{\phi_1} = \frac{z_{1lobes}}{z_{2lobes}} \qquad (8)$$

where z_{1lobes}, z_{2lobes} are the helical lobes numbers for the two worms (z_{1lobes}=2 and z_{2lobes}=3).

The gearing kinematics of the two worms assume the movements:

$$x_1 = \omega_3^T(\phi_1) \cdot X_1, \qquad (9)$$

rotation of the included worm around the axis $\vec{V}_1(Z_1)(z_1)$;

$$x_2 = \omega_3^T(\phi_2) \cdot X_2, \qquad (10)$$

rotation of the including worm around the axis $\vec{V}_2, (z_2)$.

If it is defined the relative position of the fixed references systems:

$$x_2 = \theta \cdot x_1, \qquad (11)$$

where $\theta = \begin{pmatrix} \cos\theta & 0 & \sin\theta \\ 0 & 1 & 0 \\ -\sin\theta & 0 & \cos\theta \end{pmatrix}$,

so, the relative motion of the mobile reference systems $X_1Y_1Z_1$ and $X_2Y_2Z_2$ is given by transforming:

$$X_2 = \omega_3^T(\phi_2) \cdot \theta \cdot \omega_3^T(\phi_1) \cdot X_1. \qquad (12)$$

In this way, the equations of helical lobe's flanks S_{AB}, (5), and S_{BC}, (6), are given by transforming:

$$\left(\Sigma_{AB,BC}\right)_{\phi_1} \left| X_2 = \omega_3^T(\phi_2) \cdot \theta \cdot \omega_3^T(\phi_1) \cdot X_{1AB,BC} \right. \qquad (13)$$

where $X_{1AB,BC}$, $Y_{1AB,BC}$ and $Z_{1AB,BC}$ are given by the helical flanks equations (5) and (6).

The surfaces family, by transforming the (13) equations, are expressed in form:

$$\left(\Sigma_{AB,BC}\right)_{\phi_1} \left| \begin{aligned} X_2 &= [\cos\phi_2 \cdot \cos\theta \cdot \cos\phi_1 + \sin\phi_2 \cdot \sin\phi_1] \cdot X_1 + \\ &+ [-\cos\phi_2 \cdot \cos\theta \cdot \sin\phi_1 + \sin\phi_2 \cdot \cos\phi_1] \cdot Y_1 + \\ &+ [\cos\phi_2 \cdot \sin\theta] \cdot Z_1; \\ Y_2 &= [-\sin\phi_2 \cdot \cos\theta \cdot \cos\phi_1 + \cos\phi_2 \cdot \sin\phi_1] \cdot X_1 + \\ &+ [\sin\phi_2 \cdot \cos\theta \cdot \sin\phi_1 + \cos\phi_2 \cdot \cos\phi_1] \cdot Y_1 + \\ &+ [-\sin\phi_2 \cdot \sin\theta] \cdot Z_1; \\ Z_2 &= [-\sin\theta \cdot \cos\phi_1] \cdot X_1 + [\sin\theta \cdot \sin\phi_1] \cdot Y_1 + \\ &+ Z_1 \cdot \cos\theta; \end{aligned} \right. \qquad (14)$$

The equations (14) represents, consecutive, the surfaces family generated in the $X_2Y_2Z_2$ reference system by flanks S_{AB}, (5), respectively, S_{BC}, (6). The enwrapping condition of surfaces family (14) is given in form:

$$\begin{vmatrix} \dot{X}_{2\phi} & \dot{Y}_{2\phi} & \dot{Z}_{2\phi} \\ \dot{X}_{2\phi_1} & \dot{Y}_{2\phi_1} & \dot{Z}_{2\phi_1} \\ \dot{X}_{2\varphi_{i,e}} & \dot{Y}_{2\varphi_{i,e}} & \dot{Z}_{2\varphi_{i,e}} \end{vmatrix} = 0, \qquad (15)$$

for variables Φ and $\varphi_{i,e}$ – from helical flanks equations (5), (6) and $\Phi_{1,2}$ – movement parameters in generating process of including worm.

The $\varphi_{i,e}$ parameter is the generic representation for φ_e, respectively φ_i, see (1) and (2). In correlation with (15) they are defined the partial derivative:

$$\begin{aligned}
\dot{X}_{2\phi_1} &= \left\{ \begin{array}{c} \left[-sin\phi_2 \cdot cos\theta \cdot cos\phi_1 \cdot \frac{d\phi_2}{d\phi_1} - cos\phi_2 \cdot cos\theta \cdot sin\phi_1 \right] + \\ + cos\phi_2 \cdot sin\phi_1 \cdot \frac{d\phi_2}{d\phi_1} + sin\phi_2 \cdot cos\phi_1 \end{array} \right\} \cdot X_1 + \\
&+ \left\{ \begin{array}{l} sin\phi_2 \cdot \frac{d\phi_2}{d\phi_1} \cdot cos\theta \cdot sin\phi_1 - cos\phi_2 \cdot cos\theta \cdot cos\phi_1 \\ + cos\phi_2 \cdot cos\phi_1 \cdot \frac{d\phi_2}{d\phi_1} - sin\phi_2 \cdot sin\phi_1 \end{array} \right\} \cdot Y_1 - \\
&- sin\phi_2 \cdot \frac{d\phi_2}{d\phi_1} \cdot sin\theta \cdot Z_1; \\
\dot{Y}_{2\phi_1} &= \left\{ \begin{array}{l} -cos\phi_2 \cdot \frac{d\phi_2}{d\phi_1} \cdot cos\theta \cdot cos\phi_1 + sin\phi_2 \cdot cos\theta \cdot sin\phi_1 - \\ -sin\phi_2 \cdot \frac{d\phi_2}{d\phi_1} \cdot sin\phi_1 + cos\phi_2 \cdot cos\phi_1 \end{array} \right\} \cdot X_1 + \\
&+ \left\{ \begin{array}{l} cos\phi_2 \cdot \frac{d\phi_2}{d\phi_1} \cdot cos\theta \cdot sin\phi_1 + sin\phi_2 \cdot cos\theta \cdot cos\phi_1 - \\ -sin\phi_2 \cdot \frac{d\phi_2}{d\phi_1} \cdot cos\phi_1 - cos\phi_2 \cdot sin\phi_1 \end{array} \right\} \cdot Y_1 + \\
&+ \left[-cos\phi_2 \cdot \frac{d\phi_2}{d\phi_1} \cdot sin\theta \right] \cdot Z_1; \\
\dot{Z}_{2\phi_1} &= sin\theta \cdot sin\phi_1 \cdot X_1 + sin\theta \cdot sin\phi_1 \cdot Y_1.
\end{aligned} \tag{16}$$

As well, the partial derivatives regarding φ are defined:

$$\begin{aligned}
\dot{X}_{2_\varphi} &= \left[cos\phi_2 \cdot cos\theta \cdot cos\varphi_1 + sin\phi_2 \cdot sin\phi_1 \right] \cdot \dot{X}_{1_\varphi} + \\
&+ \left[-cos\phi_2 \cdot cos\theta \cdot sin\varphi_1 + sin\phi_2 \cdot cos\phi_1 \right] \cdot \dot{Y}_{1_\varphi} + \\
&+ \left[cos\phi_2 \cdot sin\theta \right] \cdot \dot{Z}_{1_\varphi}; \\
\dot{Y}_{2_\varphi} &= \left[-sin\phi_2 \cdot cos\theta \cdot cos\phi_1 + cos\phi_2 \cdot sin\phi_1 \right] \cdot \dot{X}_{1_\varphi} + \\
&+ \left[sin\phi_2 \cdot cos\theta \cdot sin\phi_1 + cos\phi_2 \cdot cos\phi_1 \right] \cdot \dot{Y}_{1_\varphi} + \\
&+ \left[-sin\phi_2 \cdot sin\theta \right] \cdot \dot{Z}_{1_\varphi}; \\
\dot{Z}_{2_\varphi} &= \left[-sin\theta \cdot cos\phi_1 \right] \cdot \dot{X}_{1_\varphi} + \left[sin\theta \cdot sin\phi_1 \right] \cdot \dot{Y}_{1_\varphi} + \\
&+ \dot{Z}_{1_\varphi} \cdot cos\theta
\end{aligned} \tag{17}$$

and, at the same time, partial derivatives regarding *Φ*:

$$\begin{aligned}
\dot{X}_{2_\phi} &= \left[cos\phi_2 \cdot cos\theta \cdot cos\phi_1 + sin\phi_2 \cdot sin\phi_1 \right] \cdot \dot{X}_{1_\phi} + \\
&+ \left[-cos\phi_2 \cdot cos\theta \cdot sin\phi_1 + sin\phi_2 \cdot cos\phi_1 \right] \cdot \dot{Y}_{1_\phi} + \\
&+ \left[cos\phi_2 \cdot sin\theta \right] \cdot \dot{Z}_{1_\phi}; \\
\dot{Y}_{2_\phi} &= \left[-sin\phi_2 \cdot cos\theta \cdot cos\phi_1 + cos\phi_2 \cdot sin\phi_1 \right] \cdot \dot{X}_{1_\phi} + \\
&+ \left[sin\phi_2 \cdot cos\theta \cdot sin\phi_1 + cos\phi_2 \cdot cos\phi_1 \right] \cdot \dot{Y}_{1_\phi} + \\
&+ \left[-sin\phi_2 \cdot sin\theta \right] \cdot \dot{Z}_{1_\phi}; \\
\dot{Z}_{2_\phi} &= \left[-sin\theta \cdot cos\phi_1 \right] \cdot \dot{X}_{1_\phi} + \left[sin\theta \cdot sin\phi_1 \right] \cdot \dot{Y}_{1_\phi} + \\
&+ \dot{Z}_{1_\phi} \cdot cos\theta,
\end{aligned} \tag{18}$$

with remark that the φ parameter become φ_e for Σ_{AB} surface and φ_i for Σ_{BC} surface.

Keeping in mind the form of equations of surfaces Σ_{AB}, (5), and Σ_{BC}, (6), then, the partial derivatives regarding φ and *Φ* are defined:

- for Σ_{AB} surface:

$$\begin{aligned}
\dot{X}_{1_{\varphi_e}} &= -r \cdot \left(sin\varphi_e \cdot cos\phi - cos\varphi_e \cdot sin\phi \right); \\
\dot{Y}_{1_{\varphi_e}} &= -r \cdot \left(sin\varphi_e \cdot sin\phi + cos\varphi_e \cdot cos\phi \right); \\
\dot{Z}_{1_{\varphi_e}} &= 0
\end{aligned} \tag{19}$$

and

$$\begin{aligned}
\dot{X}_{1\phi} &= -r \cdot cos\varphi_e \cdot sin\phi - \\
&- \left(r \cdot sin\varphi_e + R \right) \cdot cos\phi; \\
\dot{Y}_{1\phi} &= r \cdot cos\varphi_e \cdot cos\phi - \\
&- \left(r \cdot sin\varphi_e + R \right) \cdot sin\phi; \\
\dot{Z}_{1\phi} &= -p;
\end{aligned} \tag{20}$$

- for Σ_{BC} surface:

$$\begin{aligned}
\dot{X}_{1_{\varphi_i}} &= r \cdot sin\varphi_i \cdot cos\phi - r \cdot cos\varphi_i \cdot sin\phi; \\
\dot{Y}_{1_{\varphi_i}} &= r \cdot sin\varphi_i \cdot sin\phi + r \cdot cos\varphi_i \cdot cos\phi; \\
\dot{Z}_{1_{\varphi_i}} &= 0;
\end{aligned} \tag{21}$$

and

$$\begin{aligned}
\dot{X}_{1\phi} &= -\left(-r \cdot cos\varphi_i + R \right) \cdot sin\phi - \\
&- r \cdot sin\varphi_i \cdot cos\phi; \\
\dot{Y}_{1\phi} &= \left(-r \cdot cos\varphi_i + R \right) \cdot cos\phi - \\
&- r \cdot sin\varphi_i \cdot sin\phi; \\
\dot{Z}_{1\phi} &= -p.
\end{aligned} \tag{22}$$

3. Constructive solution for conical cycloid worm

3.1. Crossing profile of the cycloid worm

They are defined the references systems:

- *xyz* – fixed reference system, joined with rotation axis of base (*R*);
- $x_e y_e z_e$ – reference system joined with O_e external roulette origin;
- $x_i y_i z_i$ – reference system joined with *Oi* internal roulette origin;
- $X_1 Y_1 Z_1$ – reference system joined with generated profile;
- $X_e Y_e Z_e$ – mobile reference system joined with point *A*;
- $X_i Y_i Z_i$ – mobile reference system joined with point *B*.

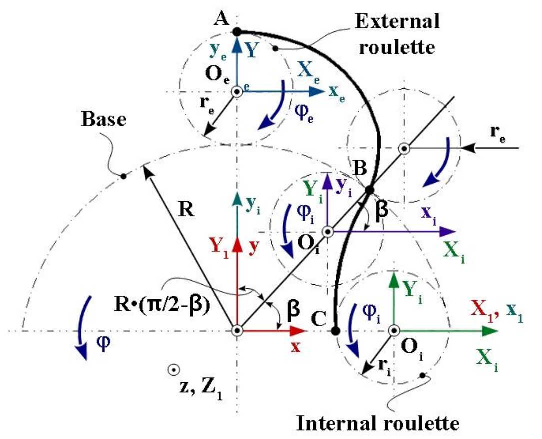

Fig. 5. *Cycloid profile of worm. Reference system*

They are defined the coordinates of points onto the roulettes which generate arcs of epicycloids and hypocycloids:

$$A\begin{cases} X_e = 0; \\ Y_e = r_e; \end{cases} \quad B\begin{cases} X_i = r_i \cdot cos\,\beta; \\ Y_i = r_i \cdot \sin\beta. \end{cases} \tag{23}$$

Also, the roulettes and base movements around axes z_e, z_i and z are defined:

$$x_e = \omega_3^T(-\varphi_e)\cdot X_e; \tag{24}$$

$$x_i = \omega_3^T(\varphi_i)\cdot X_i; \tag{25}$$

$$x = \omega_3^T(\varphi)\cdot X; \tag{26}$$

- the rolling condition of base and roulettes:

$$r_i \cdot \varphi_i = R \cdot \varphi; \tag{27}$$

$$r_e \cdot \varphi_e = R \cdot \varphi; \tag{28}$$

The matrix X_e, X_i and X are forms with coordinates of current point in mobile reference systems.

The relative positions of x_iy_i and x_ey_e reference systems regarding the xy reference system joined with base:

$$x_e = x + \begin{pmatrix} 0 \\ R + r_e \end{pmatrix}; \tag{29}$$

$$x_i = x + \begin{pmatrix} (R - r_i)\cdot cos\,\beta \\ (R - r_i)\cdot sin\,\beta \end{pmatrix}. \tag{30}$$

The relative movements results:

$$X = \omega_3(\varphi)\left[\omega_3^T(-\varphi_e)\cdot X_e + \begin{pmatrix} 0 \\ R + r_e \end{pmatrix}\right], \tag{31}$$

representing the A point movement onto the external roulette regarding the XYZ reference system of the included rotor, and

$$X = \omega_3(\varphi)\begin{bmatrix} \omega_3^T(\varphi_i)\cdot\begin{pmatrix} r_i \cdot cos\,\beta \\ r_i \cdot sin\,\beta \end{pmatrix} + \\ + \begin{pmatrix} (R - r_i)\cdot cos\,\beta \\ (R - r_i)\cdot sin\,\beta \end{pmatrix} \end{bmatrix}, \tag{32}$$

representing the movement of the B point of internal roulette, regarding the XYZ reference system.

From the movement (31) and coordinates of A point in X_iY_i reference system, (23), the equation of the epicycloids arc $\overset{\frown}{AB}$: results:

$$\overset{\frown}{AB}\left| \begin{aligned} & X = r_e \cdot cos\,\varphi \cdot sin\,\varphi_e + \\ & + \left[r_e \cdot cos\,\varphi_e + (R + r_e) \right] \cdot sin\,\varphi; \\ & Y = r_e \cdot sin\,\varphi \cdot sin\,\varphi_e + \\ & + \left[r_e \cdot cos\,\varphi_e + (R + r_e) \right] \cdot cos\,\varphi \end{aligned} \right. \tag{33}$$

and, similarly, from (32) and (23), the hypocycloid $\overset{\frown}{BC}$ equations result:

$$\overset{\frown}{BC}\left| \begin{aligned} & X = r_i \cdot cos(\beta + \varphi_i - \varphi) + \\ & + (R - r_i)\cdot cos(\varphi - \beta); \\ & Y = r_i \cdot sin(\beta + \varphi_i - \varphi) + \\ & + (R - r_i)\cdot sin(\varphi - \beta), \end{aligned} \right. \tag{34}$$

where:

$$\beta = \frac{\pi \cdot r_i}{R}; \quad r_i = r_e = r; \quad \beta = \frac{\pi}{4}, \tag{35}$$

for a worm with two lobes.

3.2. Equations of the conic helical surfaces — flanks of the included worm lobes

In figure 6 is presented the support conic surface of worm with cycloid flanks, the current radius of conic surface is R:

$$R = R_0 - p\cdot\phi\cdot tg\alpha, \tag{36}$$

with: p – helical parameter (constructive); R – radius of the frontal basis (constructive); α – angle of conic surface’s generatrix with cone’s axis

$$r=\frac{1}{4}\cdot\left(R_0-p\cdot\phi\cdot tg\alpha\right), \qquad (37)$$

for a worm with two starts.

They are defined the reference systems:

- XYZ – mobile reference system, where the frontal profile of lobe is defined – curves $\overset{\frown}{AB}$ and $\overset{\frown}{BC}$;
- $X_1Y_1Z_1$ – reference system joined with conic surface associated with included worm.

The helical surface of tooth flanks is generated in the movement:

$$X_1=\omega_3^T\left(\phi\right)\cdot X-p\cdot\phi\cdot\vec{k}\,, \qquad (38)$$

with: p – helical parameter; φ - variable angular parameter; X – matrix of current point coordinates, for curves $\overset{\frown}{AB}$ (33) and $\overset{\frown}{BC}$ (34).

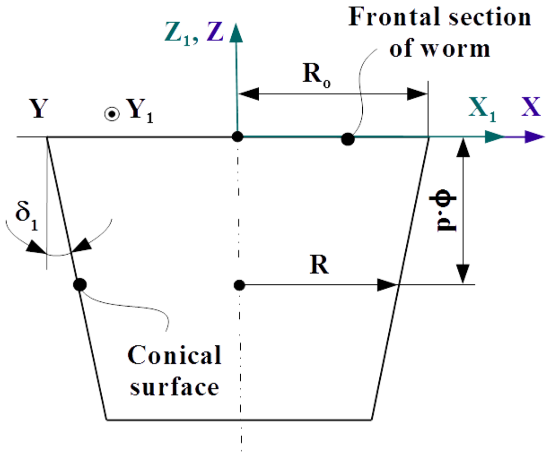

Fig. 6. *Axial section of conical surface; reference systems*

The conic helical surface generated by arc $\overset{\frown}{AB}$ is:

$$\begin{pmatrix}X_1\\ Y_1\\ Z_1\end{pmatrix}=\begin{pmatrix}\cos\phi & -\sin\phi & 0\\ \sin\phi & \cos\phi & 0\\ 0 & 0 & 1\end{pmatrix}\cdot\begin{pmatrix}r\cdot\sin\left(\varphi+\varphi_e\right)+\left(R+r\right)\cdot\sin\varphi\\ r\cdot\cos\left(\varphi+\varphi_e\right)+\left(R+r\right)\cdot\cos\varphi\end{pmatrix}-\begin{pmatrix}0\\ 0\\ p\cdot\phi\end{pmatrix} \qquad (39)$$

or, after developments:

$$\Sigma_{AB}\left|\begin{aligned}&X_1=\left[r\cdot\sin\left(\varphi+\varphi_e\right)+\left(R+r\right)\cdot\sin\varphi\right]\cdot\cos\phi-\\&-\left[r\cdot\cos\left(\varphi+\varphi_e\right)+\left(R+r\right)\cdot\cos\varphi\right]\cdot\sin\phi\\&Y_1=\left[r\cdot\sin\left(\varphi+\varphi_e\right)+\left(R+r\right)\cdot\sin\varphi\right]\cdot\sin\phi-\\&-\left[r\cdot\cos\left(\varphi+\varphi_e\right)+\left(R+r\right)\cdot\cos\varphi\right]\cdot\cos\phi\\&Z_1=-p\cdot\phi\end{aligned}\right. \qquad (40)$$

representing the epicycloids flank of included lobe of the compressor. Similarly, the equations of the hypocycloid flank, generated by curve $\overset{\frown}{BC}$ are defined, see figure 4:

$$\Sigma_{BC}\left|\begin{aligned}&X_1=r\cdot\cos\left(\beta+\varphi_i-\varphi+\phi\right)+\left(R+r\right)\cdot\\&\cdot\cos\left(\varphi-\beta+\phi\right);\\&Y_1=r\cdot\sin\left(\beta+\varphi_i-\varphi+\phi\right)+\left(R-r\right)\cdot\\&\cdot\sin\left(\varphi-\beta+\phi\right);\\&Z_1=-p\cdot\phi.\end{aligned}\right. \qquad (41)$$

Also, the equations (40) can be bring in form:

$$\Sigma_{AB}\left|\begin{aligned}&X_1=r\cdot\sin\left(\varphi+\varphi_e-\phi\right)-\\&-\left(R+r\right)\cdot\sin\left(\varphi-\phi\right);\\&Y_1=r\cdot\cos\left(\varphi+\varphi_e-\phi\right)+\\&+\left(R+r\right)\cdot\cos\left(\varphi-\phi\right);\\&Z_1=-p\cdot\phi.\end{aligned}\right. \qquad (42)$$

The definitions for r, R and β are as above. Also, there dependencies:

$$\varphi_e=\varphi_i=i\cdot\varphi,\quad \left(i=3/2\right), \qquad (43)$$

for a worm with two starts.

The condition (43) results from the arcs equality (movement of basis and roulettes):

$$\varphi\cdot R=\varphi_i\cdot r\,. \qquad (44)$$

3.3. Surfaces of the including worm

The kinematics of the rolling process for including worm flanks generating is identically with those previously analysed, for worm with circular lobes, see figure 3. In this way, the equations of the surfaces family generated by cycloid flanks, in the relative movement of conic surfaces, see (13), leads to forms (14), when the equations of the worm’s lobes are given consequently, by equations (42) for Σ_{AB} and (41) for Σ_{BC}.

In these conditions, the (14) surfaces family, in $X_2Y_2Z_2$ reference system, leads to equations depending by the independent variable parameters: Φ_1 – rotation angle of the $X_1Y_1Z_1$ reference system; Φ - angular parameter of the helical surfaces Σ_{AB}, Σ_{BC}, (41), (42); φ_e, respectively φ_i angular parameters for generating the epicycloids and hypocycloid.

So, in principle, the equations (15) are functions in form:

$$\left(\Sigma_{AB,BC}\right)_{\phi_1} \left| \begin{array}{l} X_2 = X_2\left(\phi_1, \phi, \varphi_{i,e}\right); \\ Y_2 = Y_2\left(\phi_1, \phi, \varphi_{i,e}\right); \\ Z_2 = Z_2\left(\phi_1, \phi, \varphi_{i,e}\right). \end{array} \right. \quad (45)$$

Obviously, between the Φ_1 and Φ_2 angular parameters is the dependency given by relation (8) – gearing ratio between the rotation of the included body (2 lobes) and the including body (3 lobes). The enwrapping of $\left(\Sigma_{AB}\right)_{\phi_1}$ and $\left(\Sigma_{BC}\right)_{\phi_1}$ surfaces' families is obtained associating with equations (13) the enwrapping condition (15).

The specific enwrapping condition is in form:

$$\Delta_{AB} = \begin{vmatrix} \dot{X}_{2\phi_1} & \dot{Y}_{2\phi_1} & \dot{Z}_{2\phi_1} \\ \dot{X}_{2\phi} & \dot{Y}_{2\phi} & \dot{Z}_{2\phi} \\ \dot{X}_{2\varphi_e} & \dot{Y}_{2\varphi_e} & \dot{Z}_{2\varphi_e} \end{vmatrix} = 0, \ \left(\Sigma_{AB}\right)_{\phi_1} \quad (46)$$

and, similarly, Δ_{φ_i}, for $\left(\Sigma_{BC}\right)_{\phi_1}$, when the last row of the Δ_{BC} determinant become $\dot{X}_{2\varphi_i}\ \dot{Y}_{2\varphi_i}\ \dot{Z}_{2\varphi_i}$.

The $\dot{X}_{2\phi_1}$, $\dot{Y}_{2\phi_1}$ and $\dot{Z}_{2\phi_1}$ partial derivatives are given by (20), where X_1, Y_1 and Z_1 have forms (41) for Σ_{AB} and (42) for Σ_{BC}.

Also, the partial derivatives $\dot{X}_{2\phi}$, $\dot{Y}_{2\phi}$, $\dot{Z}_{2\phi}$ and $\dot{X}_{2\varphi_{e,i}}$, $\dot{Y}_{2\varphi_{e,i}}$ and $\dot{Z}_{2\varphi_{e,i}}$ are similar with (19), respectively (20), where are defined, for Σ_{AB},

$$\begin{array}{l} \dot{X}_{1\varphi_e} = r\cdot(1+i)\cdot cos\left[\varphi_e(1+i)-\phi\right]- \\ -(R+r)\cdot i\cdot cos(i\cdot\varphi_e-\phi); \\ \dot{Y}_{1\varphi_e} = -r\cdot(1+i)\cdot sin\left[\varphi_e(1+i)-\phi\right]- \\ -i\cdot(R+r)\cdot sin(i\cdot\varphi_e-\phi); \\ \dot{Z}_{1\varphi_e} = 0, \end{array} \quad (47)$$

also,

$$\begin{array}{l} \dot{X}_{1\phi} = -r\cdot cos\left[\varphi_e(1+i)-\phi\right]+ \\ +(R+r)\cdot cos(i\cdot\varphi_e-\phi); \\ \dot{Y}_{1\phi} = r\cdot sin\left[\varphi_e(1+i)-\phi\right]+ \\ +i\cdot(R+r)\cdot sin(i\cdot\varphi_e-\phi); \\ \dot{Z}_{1\phi} = p, \end{array} \quad (48)$$

similarly, for Σ_{BC}

$$\begin{array}{l} \dot{X}_{1\varphi_i} = -(1-i)r\cdot sin\left[\beta+\phi+\varphi_i(1+i)\right]- \\ -i\cdot(R-r)\cdot sin(i\cdot\varphi_i-\beta+\phi); \\ \dot{Y}_{1\varphi_i} = (1-i)r\cdot cos\left[\beta+\phi+\varphi_i(1-i)\right]+ \\ +i\cdot(R-r)\cdot cos(i\cdot\varphi_i-\beta+\phi); \\ \dot{Z}_{1\varphi_i} = 0, \end{array} \quad (49)$$

and, at the same time,

$$\begin{array}{l} \dot{X}_{1\phi} = -r\cdot sin\left[\beta+\phi+\varphi_i(1-i)\right]- \\ -(R-r)\cdot sin(i\cdot\varphi_i-\beta+\phi); \\ \dot{Y}_{1\phi} = r\cdot cos\left[\beta+\phi+\varphi_i(1-i)\right]+ \\ +(R-r)\cdot cos(i\cdot\varphi_i-\beta+\phi); \\ \dot{Z}_{1\phi} = p, \end{array} \quad (50)$$

with: p – helical parameter of helix onto the included worm:

$$i = \frac{\varphi_e}{\varphi} = \frac{\varphi_i}{\varphi}, \quad (51)$$

from the rolling condition of roulettes (r_i, r_e) onto the base R.

For comparison of the two cases, the equality condition between the external diameters in frontal position, for the two worms with circular bulbs and with cycloid bulbs, is imposed.

4. COMPARISSON BETWEEN THE TWO CONSTRUCTIVE SOLUTIONS

They were considered worms with the same helical parameter:

- Cycloid conical worms with $r_e = r_i = 5$ mm; $R = 10$ mm;

- Worms with circular profile with $r_e = 6.5$ mm; $r_i = 18.33$ mm; $R = 10$ mm.

In both cases, the external diameter of included worm was 30 mm.

For cycloid conical worm the included worm frontal section area is 353.429 mm^2 and the including worm section area is 746.131 mm^2. So, the enclosed area is 392.702 mm^2.

For worms with circular profile the included worm frontal section is 324.081 mm^2 and the including worm section area is 703.770 mm^2. So, the enclosed area is 379.689 mm^2.

The areas enclosed between the included and including worms are presented in figure 7.a for cycloid worms and in figure 7.b for circular worms.

The difference between the enclosed areas is 13.013 mm^2.

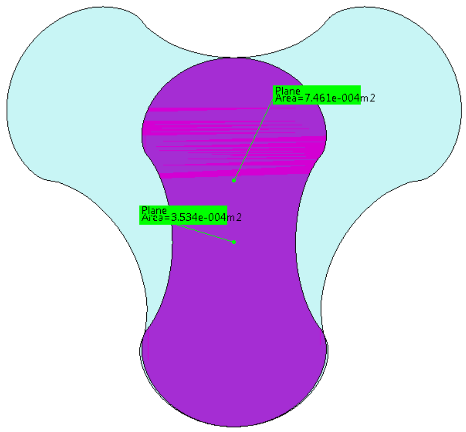

a.

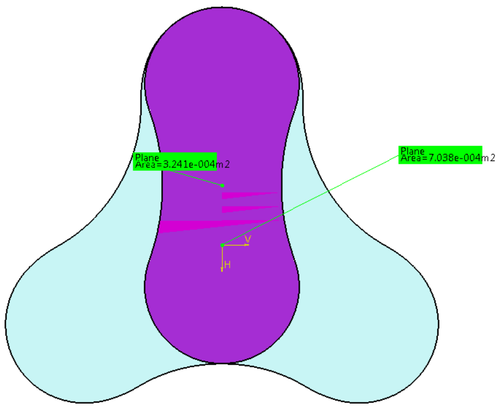

b.

Fig. 7. *Areas enclosed between the included and including worms:* ***a.*** *for cycloid worms;* ***b.*** *for circular worms*

ACKNOWLEDGEMENTS

This work was supported by a grant of the Romanian National Authority for Scientific Research and Innovation, CNCS-UEFISCDI, project number PN-III-P1-1.2-PCCDI-2017-0446 - TFIPMAIAA, Intelligent manufacturing technologies for advanced production of parts from automobiles and aeronautics industries.

4. CONCLUSIONS

It is possible to construct a worm with circular lobes, which meet the requirements for active worms of conical compressors.

The construction of worms with profile in circle arcs may solution more simple than the generatrix obtained as circles family — current solution.

The worms with circular profiles are, in principle, solutions more technologically. At the same time, the measuring possibilities are more rigorous and the generating tools are easier to make.

REFERENCES

[1] **Chang, S.,** *Cone type compressor,* US2765114A - United States Patent, Robbins & Myers, Inc., Springfield, 1956;

[2] **Dmitriev, O., Arbon, I.,** *Comparison of energy – efficiency and size of portable oil – free screw scroll compressors*, Vert Rotors U.K., Ltd. Edinburgh, U.K;

[3] **Dmitriev, O., Arbon, I.,** *A compact water-injected screw compressor with high volumetric efficiency*, 13th, European Fluid Machinery Congress, The Hague, The Netherlands, 2016;

[4] **Dmitriev, O., Tabota, E.,** *A working conical screw compressor*, 12th, European Fluid Machinery Congress, Edinburgh, U.K., 2014;

[5] **Dmitriev, O., Tabota, E., Arbon, I.,** *A miniature Rotary Compressor with a 1:10 compression ratio*, 10P Conf. Ser: Mater. Sci. Eng. 90012055, 2015;

[6] **Litvin, F.L.,** *Theory of Gearing*, Reference Publication, 1212, NASA, Sci-entific and Technical Information Division, Washington D.C., 1984;

[7] **Oancea, N.,** *Generarea suprafeţelor prin înfăşurare (Surfaces generation by winding),* Vol. I-III, Galaţi University Press, 2004, ISBN 973-627-170-4, ISBN 973-627-107-2 (vol. I), ISBN 973-627-176-6 (vol II), ISBN 973-627-239-7 (vol III);

[8] **Baroiu, N., Păunoiu, V., Teodor, V.G., Susac, F., Oancea, N.,** *Geometrical analysis, for rapid prototyping, of the compressor's helical conic rotor model*, MATEC Web Conf., Volume 178, 2018, 22nd International Conference on Innovative Manufacturing Engineering and Energy - IManE&E 2018;

[9] **Teodor, V.,** *Contributions to developing a method of profiling tools that generate by enveloping*, Doctoral Thesis, “Dunărea de Jos” University of Galaţi, 2005.